Study on the Dynamic Characteristics of Spent Fuel Pool Considering Liquid Sloshing

Wenting Bai[1,2,a], Guozhong Feng[3,b*], Xuechuan Han[1,2,c], Yu zhu[1,d], Jiachang Wang[1,e], Yongyi Fan[1,f]

[1]College of Urban Geology and Engineering, Hebei GEO University, Hebei 050031, China
[2]Hebei Technology Innovation Center for Intelligent Development and Control of Underground Built Environment, Hebei GEO University, Hebei 050031, China
[3]China Nuclear Power Engineering Co., Ltd. Hebei Branch, Hebei 050000, China

[a]bwenting@163.com, [b]gz_fung@163.com, [c]tshanxuechuan@126.com, [d]15733181123@163.com, [e]18833120798@163.com, [f]a1303901587@163.com
*Corresponding author

Abstract. In the past decade, multiple accidents related to spent fuel pools have occurred consecutively, a large part of which are related to the large sloshing of the liquid inside the spent fuel pool under earthquake action. In order to study the influence of liquid sloshing on the dynamic characteristics of spent fuel pools in nuclear power plants, the modal, liquid sloshing height, and response spectrum of spent fuel pools with different liquid to liquid ratios were analyzed under seismic action using the Coupled Eulerian-Lagrangian analysis method. The analysis results showed that as the liquid content increases, the stiffness of the liquid structure coupling system tends to decrease. When the planar shape of the pool was fixed, under the same seismic excitation, regardless of the liquid content in the pool, the maximum height of liquid sloshing was basically the same. When the liquid content in the spent fuel pool is 4/5, the seismic performance and functional utilization of the pool are good. The liquid exerts a damping effect on the wall of the spent fuel pool. As the liquid to water ratio increases, thinner pool walls are more affected by water sloshing effects compared to thicker pool walls.

Keywords: spent fuel pool, fluid solid coupling, dynamic analysis, liquid sloshing height, response spectrum

1 Introduction

Nuclear energy is a clean, efficient, and resource rich energy source, but its utilization also comes with high risks. In 2011, the Fukushima nuclear power plant accident in Japan was the world's first spent fuel plant explosion accident. The main reason was that the detection equipment used for the spent fuel pool failed to detect the water level of the pool in a timely and accurate manner under the action of an earthquake, resulting in a lack of information on the safe storage of the spent fuel pool [1]. This

Y. Zhang et al. (eds.), *Proceedings of the 2024 10th International Conference on Architectural, Civil and Hydraulic Engineering (ICACHE 2024)*, Advances in Engineering Research 259,
https://doi.org/10.2991/978-94-6463-658-1_90

caused a series of chain reactions that endangered the lives and property safety of Japanese and even global people. In March 2022, a 7.4-magnitude earthquake occurred in Japan, causing the shutdown of spent fuel pools in some units of the Fukushima nuclear power plant. In January 2024, a 7.6-magnitude earthquake struck the Noto Peninsula in Japan, causing water overflow in the spent fuel pools of multiple nuclear power plants such as Shiga Nuclear Power Plant and Kashiwazaki Kariwa Nuclear Power Plant. A series of accidents involving spent fuel pools have raised widespread public concern about the safety of nuclear energy operations. In terms of fluid structure coupling research related to nuclear power safety, Sakurai studied the effect of components in a large pool of LMFBR (breeder reactor) on the sloping wave heights [2]. Eswaran used a partitioned strong fluid-structure coupling to simulate the liquid sloshing in fuel storage bays of advanced reactors subject to earthquake loading. Analysis shows that if liquid oscillation cannot be effectively controlled, the shaking of the liquid in the storage bays may lead to water overflow or significant dynamic stress, resulting in structural damage [3]. Ricciardi and Mishra analyzed the impact of fluid-structure coupling on the internal pack of a storage pool [4-5]. Chinese scholars have also conducted extensive research [6-11], but few have studied spent fuel pools. Previous research on spent fuel pools has mainly focused on enhancing monitoring and emergency response plans. This article focuses on the modal characteristics of the fluid-structure coupling system in spent fuel pools, the liquid sloshing height, and the floor response spectrum. The purpose of the analysis is to study the dynamic characteristics of the spent fuel pool under the action of liquid sloshing, in order to provide design recommendations for the ancillary equipment installed on the pool wall.

2 Plan Layout and Load Case Design of Spent Fuel Pool

2.1 Plan Layout of Spent Fuel Pool

A spent fuel pool refers to a pool of water used in nuclear facilities such as a nuclear power plant to store spent fuel, which plays a role in cooling the spent fuel and shielding radiation.

The layout of the spent fuel pool studied in this article is shown in Figure 1. The wall thickness of the pool is uneven, with W1 having a wall thickness of 1.44m and W2 having a wall thickness of 2.04m. The length, width, and height of the pool are 17.20m × 11.54m × 20m.

2.2 Load Case Design

In order to study the influence of dynamic characteristics of water pool wall due to the liquid content, four operating conditions with different liquid to height ratio (the ratio of liquid height to pool height) were set up. The specific experimental load cases are shown in Table 1 and Figure 2.

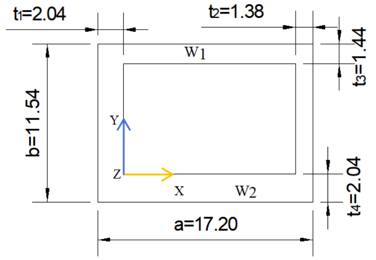

Fig. 1. Plan layout of spent fuel pool

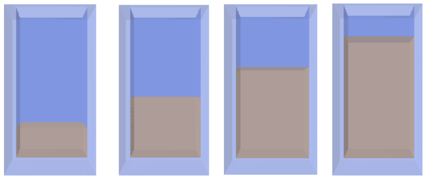

Fig. 2. Experimental load cases

Table 1. Experimental load cases

	Case 1	Case 2	Case 3	Case 4
Liquid to height ratio	1/5	2/5	3/5	4/5

3 Analysis Methods and Modeling

3.1 Analysis Methods

This study needs to consider the fluid-structure coupling between the water in the spent fuel pool and the pool wall, the Coupled Eulerian-Lagrangian analysis (CEL) method in ABAQUS/Explicit is adopted. It is an explicit dynamic analysis method. The core advantages of this method include the ability to effectively simulate fluid structure interactions, dealing with complex physical phenomena and improving the efficiency of numerical calculations [12].

3.2 Modeling

The pool structure adopts C3D8R element and C30 reinforced concrete materials, with material characteristics shown in Table 2. The liquid adopts Euler element EC3D8R, the liquid is ordinary water, and the material characteristics are shown in Table 3. The overall mesh of the spent fuel pool and liquid is shown in Figure 3. The schematic diagram of the pool and liquid mesh division is shown in Figure 4.

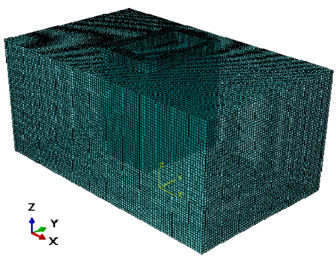

Fig. 3. The overall mesh of the spent fuel pool and liquid

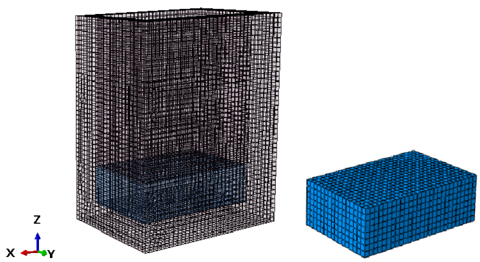

Fig. 4. The pool and liquid mesh division

Table 2. Parameters of reinforced concrete

ρ (kg/m^3)	E (N/m^2)	ν	f_{tk} (Pa)	f_t (Pa)	f_{ck} (Pa)	f_c (Pa)
2500	3.0E+06	0.3	2.01E+06	1.43E+06	20.1E+06	14.3E+06

Note: ρ is Density. E is elastic modulus. ν is Poisson's ratio. f_{tk} is standard value of axial tensile strength. f_t is design value of axial tensile strength. f_{ck} is standard value of axial compressive strength. f_c is design value of axial tensile strength.

Table 3. Parameters of liquid

Density (kg/m^3)	Viscosity coefficient ($N·s/m^2$)	Sound velocityC$_0$ (m/s)	State equation	U_S-U_P curve slope S	Gamma
1000	0.001	1483	Eos	0	0

4 Seismic Input

This article mainly studies the changes in the dynamic characteristics of the pool wall under earthquake loading due to the action of water inside the pool. The seismic waves used are El Centro triaxial seismic waves, with a time interval of 0.01 seconds. The original data shows a seismic motion duration of 91.4 seconds.

According to reference [13], the effective duration of input seismic motion should exceed 5 times the natural vibration period of the structure, and the starting and ending points should be set based on 10% of the maximum peak value, taking the first 30 seconds of the duration of the seismic motion. Calibrate the peak values in the EW direction as 0.531g, NS direction as 0.532g, and UP direction as 0.664g. The acceleration time history curve after seismic wave calibration is shown in Figures 5-7.

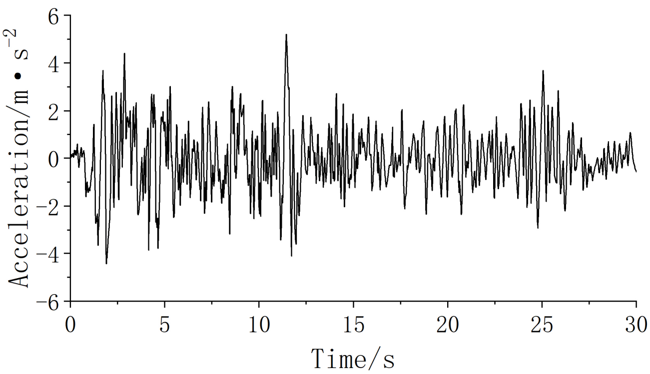

Fig. 5. EW-direction acceleration time history of El Centro

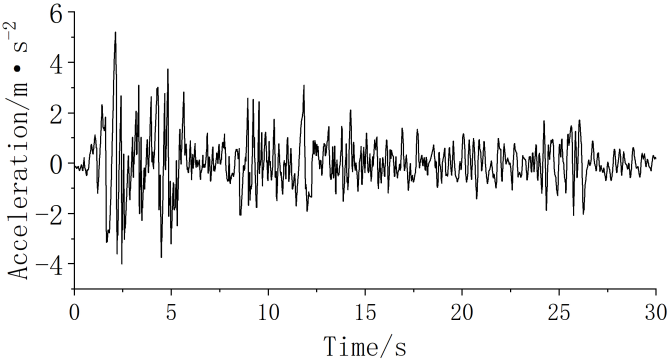

Fig. 6. NS-direction acceleration time history of El Centro

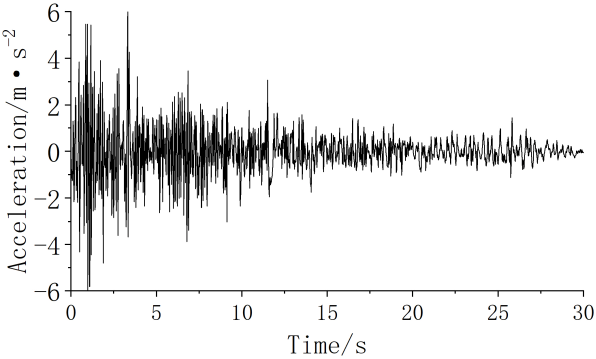

Fig. 7. UP-direction acceleration time history of El Centro

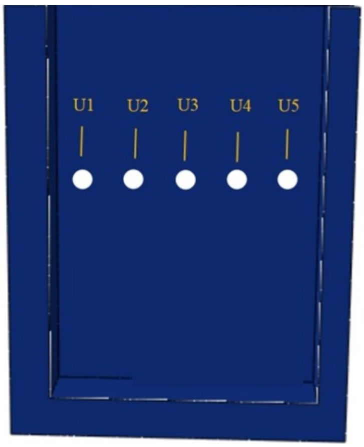

Fig. 8. Schematic diagram of node positions on the pool wall

5 Results Analysis

5.1 Node Coordinates

Take out 5 points along the pool wall W1 and pool W2 at the same horizontal height. The schematic diagram of the node position output of the pool wall is shown in Figure 8, and the parameters for node location are shown in Table 4, with the coordinate system shown in Figure 1.

Table 4. Parameters for Node Location

Node number	N：13967	N：14318	N：14669	N：15020	N：15371
Symbol	U_1	U_2	U_3	U_4	U_5
Coordinate(m)	(0.07, 0, 17)	(2.68, 0, 17)	(5.36, 0, 17)	(8.04, 0, 17)	(10.72, 0, 17)

5.2 Modal Analysis

Dry mode refers to the natural vibration frequency of a structure without considering fluid effects. Dry mode analysis is usually used for preliminary structural design and evaluation, providing reference for the basic dynamic characteristics of the structure. Correspondingly, the wet mode considers the interaction between the structure and its surrounding fluid, especially when the fluid has a significant impact on the dynamic characteristics of the structure. Wet modal analysis can help identify the vibration frequency of a structure that changes due to fluid action, and is the basis for conducting complex fluid-structure coupling analysis. Table 5 shows the first 10 modes of dry mode and wet mode of the spent fuel pool.

Table 5. Dry and wet modes

Order	Dry mode (Hz)	Wet mode (Hz)			
		liquid to height ratio 1/5	liquid to height ratio 2/5	liquid to height ratio 3/5	liquid to height ratio 4/5
1	10.553	10.534	10.395	9.9669	9.2609
2	13.765	13.738	13.627	13.286	12.625
3	14.832	14.787	14.542	13.955	13.112
4	15.968	15.995	16.251	16.646	16.609
5	22.689	22.681	22.58	21.879	21.875
6	24.080	24.139	23.088	22.656	22.528
7	28.650	28.566	27.787	26.724	25.41
8	29.852	29.385	28.64	28.44	27.917
9	37.779	37.088	32.41	31.306	28.418
10	38.713	37.88	35.598	33.51	31.989

From Table 5, it can be seen that as the liquid to height ratio increases, the frequency of the fluid-solid coupling system decreases, indicating that its stiffness gradually decreases and the fluid-solid coupling system gradually becomes flexible. This is beneficial for the internal system of nuclear power plants built on bedrock, which can effectively avoid resonance caused by similar frequencies in the site and structures.

5.3 Analysis of Liquid Sloshing Height

Observe the sloshing of liquid by extracting the nodal displacement of the sloshing surface of the fluid. The sloshing of the liquid is shown in Figures 9 to 12.

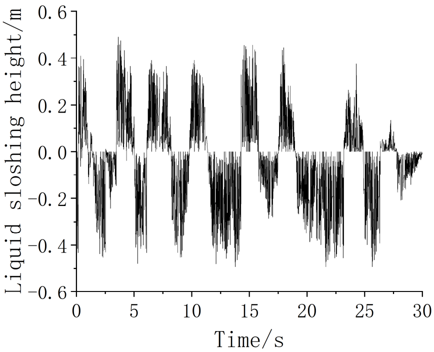

Fig. 9. Liquid sloshing at a liquid to height ratio of 1/5

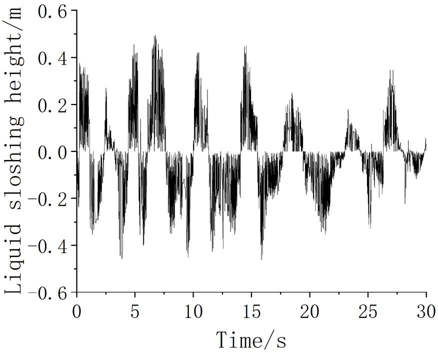

Fig. 10. Liquid sloshing at a liquid to height ratio of 2/5

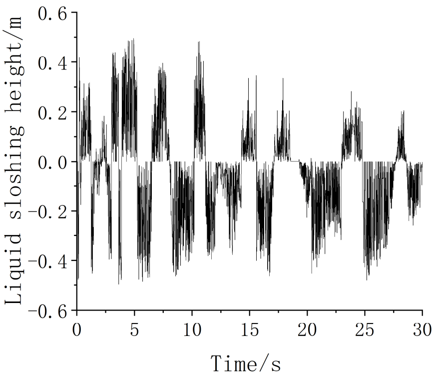

Fig. 11. Liquid sloshing at a liquid to height ratio of 3/5

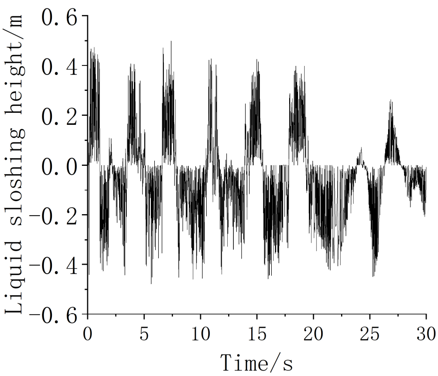

Fig. 12. Liquid sloshing at a liquid to height ratio of 4/5

As shown in Figures 8-11, under four experimental load cases with liquid to height ratios of 1/5 to 4/5, the liquid sloshing is significant in the first twenty seconds. As the acceleration amplitude decreases, the sloshing height of the liquid gradually decreases. To further observe and analyze, the maximum sloshing height of the liquid level will be statistically analyzed, as shown in Table 6.

Table 6. Statistics of maximum sloshing height on liquid surface

Liquid to height ratios	1/5	2/5	3/5	4/5
Time (s)	3.63	6.67	4.93	7.40
Sloshing height (m)	0.491	0.494	0.496	0.499

The statistical results in Table 6 indicate that when the planar shape of the pool is fixed, under the same seismic excitation, regardless of the liquid content in the pool, the maximum sloshing height is basically the same, except for differences in the time points of occurrence.

5.4 Reaction Spectrum Analysis

When calculating the floor response spectrum, the frequency increment should be adopted according to Table 7, and each peak related to the structural frequency should be widened by 0.15 times the frequency of the structure. The widened peak is determined by a straight line parallel to the original spectral peak segment [14].

Table 7. Frequency Increment of Reaction Spectrum（Hz）

Frequency range	0.2~3.0	3.0~3.6	3.6~5.0	5.0~8.0	8.0~15.0	15.0~18.0	18.0~22.0	22.0~33.0
Frequency increment	0.10	0.15	0.20	0.25	0.50	1.00	2.00	3.00

Corresponding to the distribution of nodes at the same height in Table 4 and Figure 8, Figures 13 to 22 show the envelope spectrum in the normal direction perpendicular to the pool wall with damping ratios of 0.02, 0.03, 0.04, 0.05, 0.07, and 0.1 under five load cases of no water and different liquid to height ratios.

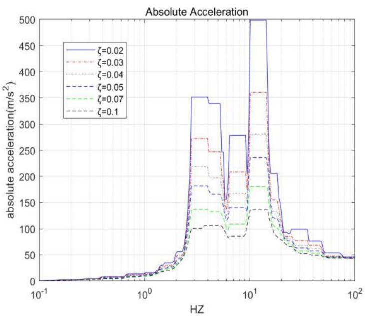

Fig. 13. Broaden envelope spectrum of W_1 without liquid

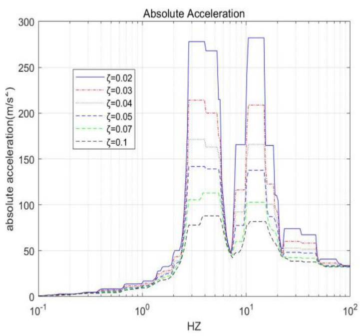

Fig. 14. Broaden envelope spectrum of W_2 without liquid

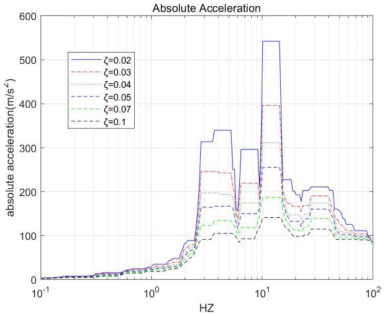

Fig. 15. Broaden envelope spectrum of W_1 at a liquid to height ratio of 1/5

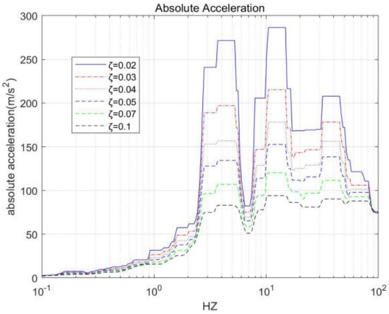

Fig. 16. Broaden envelope spectrum of W_2 at a liquid to height ratio of 1/5

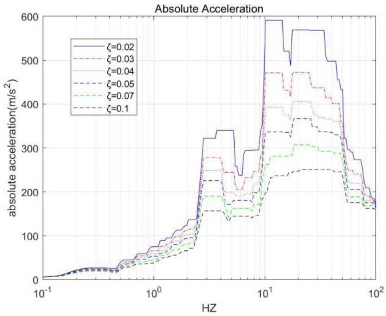

Fig. 17. Broaden envelope spectrum of W_1 at a liquid to height ratio of 2/5

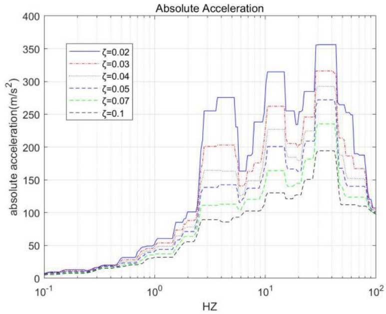

Fig. 18. Broaden envelope spectrum of W_2 at a liquid to height ratio of 2/5

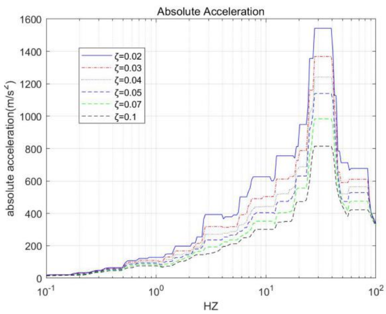

Fig. 19. Broaden envelope spectrum of W_1 at a liquid to height ratio of 3/5

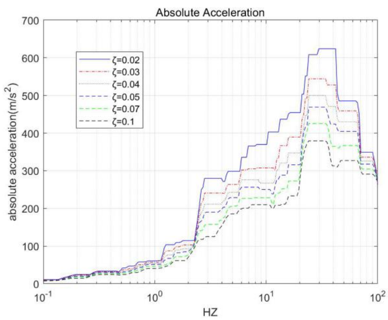

Fig. 20. Broaden envelope spectrum of W_2 at a liquid to height ratio of 3/5

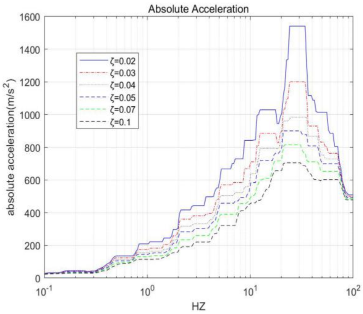

Fig. 21. Broaden envelope spectrum of W_1 at a liquid to height ratio of 4/5

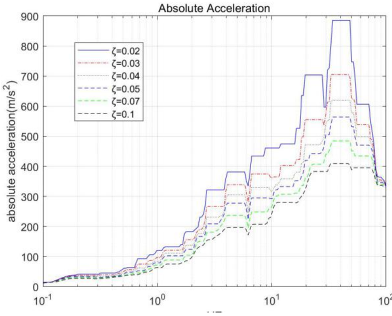

Fig. 22. Broaden envelope spectrum of W_2 at a liquid to height ratio of 4/5

In order to simplify the analysis, a fluid structure coupling amplification factor AFSI is set, which is the ratio of the maximum amplitude of the floor response spectrum to the peak amplitude of the input seismic motion. The statistical results are shown in Table 8.

Table 8. Normal Direction A_{FSI}

liquid to height ratio / pool wall	0 (without liquid)	1/5	2/5	3/5	4/5
W_1 (1.44m)	11.585	5.742	4.075	4.307	3.683
W_2 (2.04m)	8.844	7.387	4.109	5.828	4.206

(1)According to Table 8, it can be seen that in the output results of the normal direction floor response spectrum, the A_{FSI} value shows a similar amplification trend with the increase of the liquid to height ratio for different wall thicknesses of pool walls W_1 and W_2. As the filling height changes, the amplification factor first decreases, then increases, and then decreases again, indicating that the presence of water has a good impact on the seismic performance of the pool. This effect is most significant when the liquid to height ratio of the pool is about 2/5 and 4/5. Based on the statistical results of the maximum sloshing height of the liquid surface in Table 3, the maximum wave height of 0.5m is lower than the height from the water surface to the upper end of the pool wall, which can avoid overflow accidents. Considering the full utilization of the volume of the spent fuel pool, combined with the analysis of the dynamic performance and wave height mentioned above, it is comprehensively determined that the seismic performance and functional utilization of the pool are good when the liquid content of the spent fuel pool is 4/5.

(2) As the liquid to height ratio increases, the thinner pool wall W_1 is more affected by the sloshing effect of liquid on the pool wall compared to the thicker W_2.

(3)When the liquid content height of the spent fuel pool is lower than half of the total height of the pool structure, regardless of the wall thickness W_1 or W_2, due to the fluid-structure coupling effect, the dynamic amplification effect of the pool wall gradually decreases along the normal and horizontal tangential directions of the pool wall. When the liquid content height of the spent fuel pool is higher than half of the total height of the pool structure, the damping effect of the liquid in the normal direction is more significant than that in the tangential direction, and the reduction ratio of the dynamic amplification effect in the normal direction is more significant.

(4)Compared with the normal and tangential broadening envelope spectrum output results of the W_1 (wall thickness 1.44m) and W_2 (wall thickness 2.04m) pool walls, the amplification factor of fluid structure coupling gradually increases with the increase of water level in W_2 pool wall, and the dominant frequency of the broadening spectrum is relatively single. Therefore, when not considering the seismic isolation and damping measures of the ancillary equipment, it is advisable to arrange the ancillary equipment on the thinner side of W_1 as much as possible; when considering seismic isolation measures, due to the relatively single frequency on the thicker W_2 side, it is possible to use fixed frequency seismic isolation bearings to reduce the seismic effects of ancillary equipment and place the ancillary equipment on the W_2 side.

The horizontal tangential and vertical response spectra exhibit similar properties.

6 Conclusion

(1) As the liquid content increases, the stiffness of the liquid structure coupling system tends to decrease.

(2) when the planar shape of the pool is fixed, under the same seismic excitation, regardless of the liquid content in the pool, the maximum sloshing height is basically the same, except for differences in the time points of occurrence.

(3) When the liquid content in the spent fuel pool is 4/5, the seismic performance and functional utilization of the pool are good.

(4) The liquid exerts a damping effect on the wall of the spent fuel pool.

(5) As the liquid to water ratio increases, thinner pool walls are more affected by water sloshing effects compared to thicker pool walls.

The seismic design of ancillary equipment on the pool wall can be considered in two situations. When not considering the seismic isolation and damping measures of the ancillary equipment, it is advisable to arrange the ancillary equipment on the thinner side as much as possible; when considering seismic isolation measures, due to the relatively single frequency on the thicker side, it is possible to use fixed frequency seismic isolation bearings to reduce the seismic effects of ancillary equipment and place the ancil-lary equipment on the thicker side.

Acknowledgments

This work was supported by the Natural Science Foundation of Hebei Province (No. E2021403012).

References

1. NRC Order EA-12-051, (2012). To Modify Licenses with Regard to Reliable Spent Fuel Pool Instrumentation. NRC.
2. Sakurai, A. , Masuko, Y. , Kurihara, C. , Ishihama, K. , Yashiro, T. , & Chang, Y. W. , et al. (1989). Seismic sloshing experiments of large pool-type fast breeder reactors. Nuclear Engineering and Design, 113(3), 423-433.
3. Eswaran, M. , & Reddy, G. R. . (2016). Liquid sloshing in fuel storage bays of advanced reactor subjected to earthquake loading. Procedia Engineering, 144, 1278-1285.
4. Ricciardi, G. , Kang, H. S. , Oh, D. S. , & Lee, K. H. . (2021). Dynamic modeling of spent fuel rack pool subjected to seismic excitation considering fluid-structure interaction. *Journal of pressure vessel technology*(6), 143.
5. Mishra, V. K. , Panda, S. K. , Sen, B. , Maiya, M. P. , & Rao, B. P. C. . (2022). Numerical analysis of forced convection heat transfer in a nuclear fuel storage vault. *International Journal of Thermal Sciences, 173*, 107429-.
6. Gou Hongliang, & Li Yuchun. (2018). Experimental and theoretical identifications of the first sloshing modal parameters for the annular tanks with inclined bottom. *Industrial Construction, 48*(12), 6.
7. Li Jianbo, Yang Bo, Li Zhiyuan, & Ding Zhixin. (2022). Distributed Mass Calculation Model of Special-shaped Tank in Nuclear Power Project Based on CAS Method. *ENGINEERING MECHANICS, 41*(2), 160-170, 193.
8. Li Nan, & Han Zhi. (2015). Combined Mass-spring Model Used to Simulate Sloshing of Fluid in CEFR Sodium Storage Tank. *Atomic Energy Science and Technology, 49*(9), 6.
9. Liu, Y. , Deng, C. , Lu, D. , Cao, Q. , & Zhou, Y. . (2021). The fluid-structure interaction effect on seismic response of double cap1400 spent fuel storage racks. *Nuclear engineering and design*(Dec.), 384.
10. Deng, C. , Lu, D. , Liu, Y. , & Zhao, F. . (2022). Computational method for the added mass of fluid imposed on spent fuel storage racks considering three-dimensional flow. *Annals of Nuclear Energy*.
11. Lu, D. , Wang, Y. , & Jiang, L. J. . (2023). Experiments on fluid-structure interaction dynamic response of a new free-standing spent fuel storage basket. *Progress in nuclear engergy, 165*(Nov.), 104908.1-104908.12.
12. ABAQUS Inc. (2013). ABAQUS analysis user's manual. Providence, RI: Dassault Systems.
13. The state bureau of quality and technical supervision. (2012). *GB50191-2012 Code for seismic design of special strictures.* China Planning Press.
14. The state bureau of quality and technical supervision. (2019). *GB50267-2019 Seismic Design Standards for Nuclear Power Plants.* China Planning Press.